

Stanislav Bartoň

Dynamics of an artificial slope

In: Jan Chleboun and Pavel Kůs and Petr Přikryl and Miroslav Rozložník and Karel Segeth and Jakub Šístek (eds.): Programs and Algorithms of Numerical Mathematics, Proceedings of Seminar. Hejnice, June 21-26, 2020. Institute of Mathematics CAS, Prague, 2021. pp. 9–20.

Persistent URL: <http://dml.cz/dmlcz/703096>

Terms of use:

Institute of Mathematics of the Czech Academy of Sciences provides access to digitized documents strictly for personal use. Each copy of any part of this document must contain these *Terms of use*.



This document has been digitized, optimized for electronic delivery and stamped with digital signature within the project *DML-CZ: The Czech Digital Mathematics Library*
<http://dml.cz>

DYNAMICS OF AN ARTIFICIAL SLOPE

Stanislav Bartoň

Opole University of Technology,
Faculty of Electrical Engineering, Automatic Control and Informatics,
Prószkowska 76, 45-758 Opole, Poland
s.barton@po.opole.pl

Abstract: The slope shape is replaced by a 3D regression function which corresponds with high precision to the position of several hundred points which were determined on the surface of the slope body. The position of several points was repeatedly measured for several years. The time changes in the position of these points were used to create regression functions that describe vertical movements, *slope settlement* and horizontal movements, *slope movement*. The model results are presented in the form of mathematical relationships and visualized in the program Maple environment.

Keywords: nonlinear regression, mathematical modelling, visualisation, vector field, Maple

MSC: 62J02, 37C10, 65D17

1. Introduction

The artificial slope was created as a surface cover for the municipal waste landfill in Štěpánovice, Klatovy district.

Geographical coordinates and an altitude of 261 points were measured on the slope surface. Furthermore, the coordinates of six stationary *reference* points in the vicinity of the slope were determined. Fifteen *moving* points were selected on the hill, the position of which compared to the reference points was repeatedly determined twice a year for five years. The task was to find out whether the slope does not slide – that is, the moving points on the slope surface move in the direction of the slope or whether the slope does not move – in this case the moving points would move in the direction of the subsoil slopes. The new material is delivered and stored behind the right edge of the slope perimeter.

The Maple symbolic algebra program was used for all calculations and graphical outputs. Given the scope of this publication, it is not possible to state the whole calculation procedure here. Therefore, Maple commands will be listed here only for essential parts of the solution. Otherwise, the solution procedure will be described only verbally.

2. Mathematical model of slope shape

2.1. Regression function describing the shape of the slope

First it is necessary to convert the geographical coordinates in the form $[\lambda_k, \phi_k, h_k]$, $k = 1..261$, where λ = longitude, ϕ = latitude and h = altitude, to the rectangular coordinates $[x_k, y_k, h_k]$. The plane $h = 0$ of this coordinate system is the tangent plane of the Krasovsky ellipsoid, see [1], at a point which is the arithmetic mean of the coordinates λ and ϕ . The positive direction of the y axis is oriented to the north.

As a regression function for the description of the slope surface $h = f(x, y)$, it is perfect

$$h \equiv f(x, y) = K + \exp\left(-\sum_{i=0}^8 \left(x^i \sum_{j=0}^{8-i} y^j a_{i,j}\right)\right), \quad (1)$$

which is non-linear with respect to the coefficients $a_{i,j}$. These coefficients must be determined using the Gauss-Newton iteration method, see [2]. The initial values of the coefficients can be calculated by linearising the equation (1), if $K = 0$ is placed and the rectangular coordinates $[x_k, y_k, h_k]$ of the points focused on the slope surface are substituted for $[x, y, h]$,

$$\ln(h_k) = \sum_{i=0}^8 \left(x_k^i \sum_{j=0}^{8-i} y_k^j a_{i,j}\right). \quad (2)$$

The initial values of the coefficients $a_{i,j}$ can be determined from the equation (2) using the least squares method.

The final values of the coefficients from the equation (1) are calculated after 73 iteration steps. During the iteration, the size limitation of the correction members ΔA_c was used in the form of:

$$\Delta A_c = \frac{\Delta A}{\sqrt{\left(\frac{\epsilon}{100}\right)^2 + 1}}, \text{ where } \begin{cases} \Delta A = [\Delta a_{i,j}]_{i=0..8, j=0..8-i} & \text{vector of} \\ & \text{the corrections of } a_{i,j} \\ \epsilon = \sqrt{\sum_{i=0}^8 \left(\sum_{j=0}^{8-i} a_{i,j}^2\right)} & \text{quadratic norm of the corrections} \\ & \text{of the vector of the corrections} \end{cases} \quad (3)$$

The agreement between the measured heights and the heights calculated according to the equation (1) is excellent. The coefficient of determination reached the value $R^2 = 0.9995$ and the analysis of variance calculated by the ANOVA method gives the value $p = 0.9996$.

The resulting 3D regression function is shown in Figure 1. The points defining the shape of the surface are shown by crosses, the moving points are shown by small squares and black, almost invisible thick lines show the differences between the measured and calculated heights.

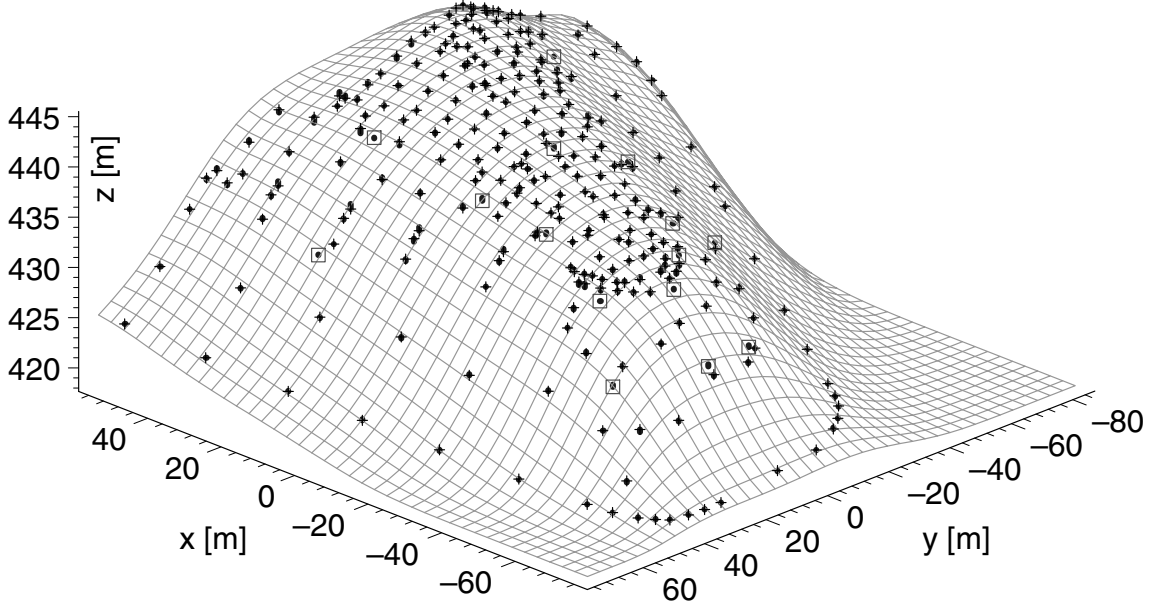


Figure 1: Regression function, measured points, moving points and differences.

2.2. Determination of the perimeter of the slope

All points were first transformed into the plane $h = 0$, i.e. $[x_k, y_k, h_k] \rightarrow [x_k, y_k, 0]$. The points on the perimeter of the hull were determined using an Incremental convex hull algorithm, *ICHA*, see [3]. After that, the convex perimeter was changed to concave using the author's algorithm. The basic principle of this algorithm is:

1. Remove all points on the slope that make up the perimeter. A set of PL points is created.
2. For each line segment LS_i that forms the perimeter, find all points from PL for which the heel of the perpendicular running from PL_j to LS_i is its own point. A set of PF points is created.
3. If the angle subtended by the lines passing through the endpoints of line segment LS_i and point PF_j is greater than the specified value, replace the line segment LS_i with two line segments that have a common point PF_j and endpoints identical with line segment LS_i .
4. Remove the PF_i point from the PF set.
5. Repeat the entire procedure until the PF set is empty.

The resulting convex perimeter after *ICHA* is shown in Figure 2 on the left. The concave perimeter, after using the author's algorithm, is shown in Figure 2 on the right. Solid circles show the points that make up the convex perimeter. The points that change the convex perimeter to concave are shown by empty circles. A cross indicates the points inside the perimeter.

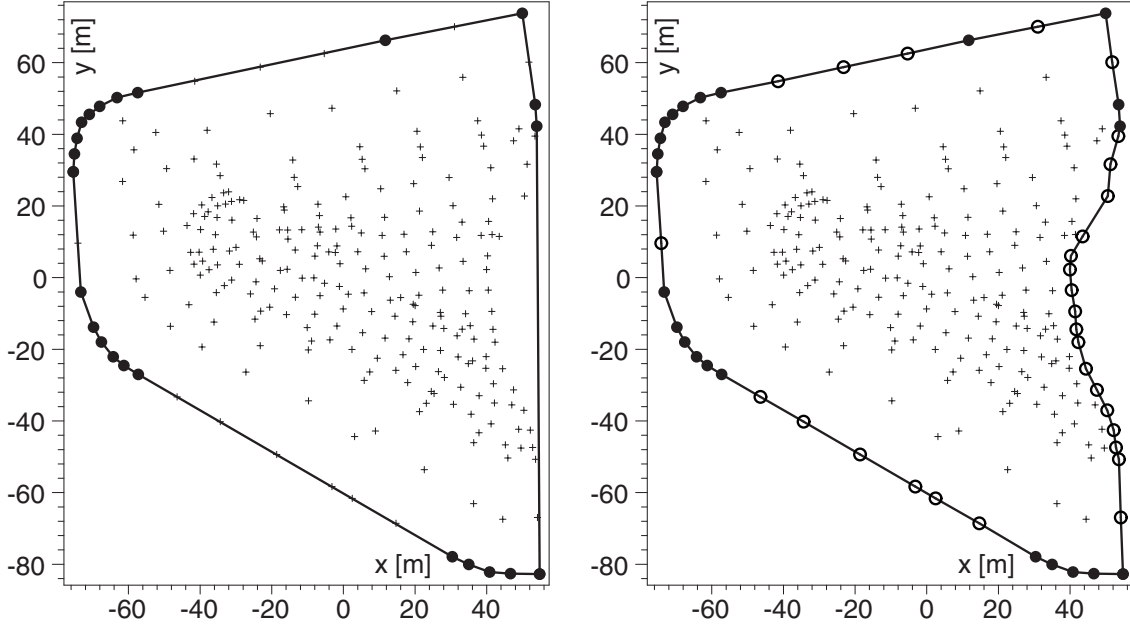


Figure 2: Convex perimeter – left and concave perimeter – right.

2.3. Triangulation

Maple cannot work with finding a curve that is created by the intersection of two surfaces. Therefore, it is not possible to limit the area showing the slope surface by a curve that results in the intersection with the surface describing the shape of the subsoil. In this case, it is possible to draw the shape of the slope using triangulation accurately because Maple can accurately display a triangle in space.

The triangulation procedure is shown in Figure 3. The basis is the circumferential curve of the slope, projected into the plane xy , including the points that define it. A regular network of right triangles is formed inside this curve. The length of the perpendicular of the triangle is chosen to correspond to the smallest distance of the two adjacent points forming the circumference, see Figure 3 on the left.

In the second step, the points of the network that are closest to the points defining the circuit are moved to these points. The remaining points of the perimeter of the triangular network are moved to the corresponding positions on the lines that make up the perimeter. See Figure 3 in the middle.

In the last step, those triangles that are too large are divided into four smaller ones, see Figure 3 on the right.

The spatial representation of triangulation is shown in Figure 4.

2.4. Shape of the subsoil

The function,

$$h = 425.61 + 0.000106 x^2 + 0.0000113 y^2 + 0.074770 x - 0.049936 y - 0.000260 xy \quad (4)$$

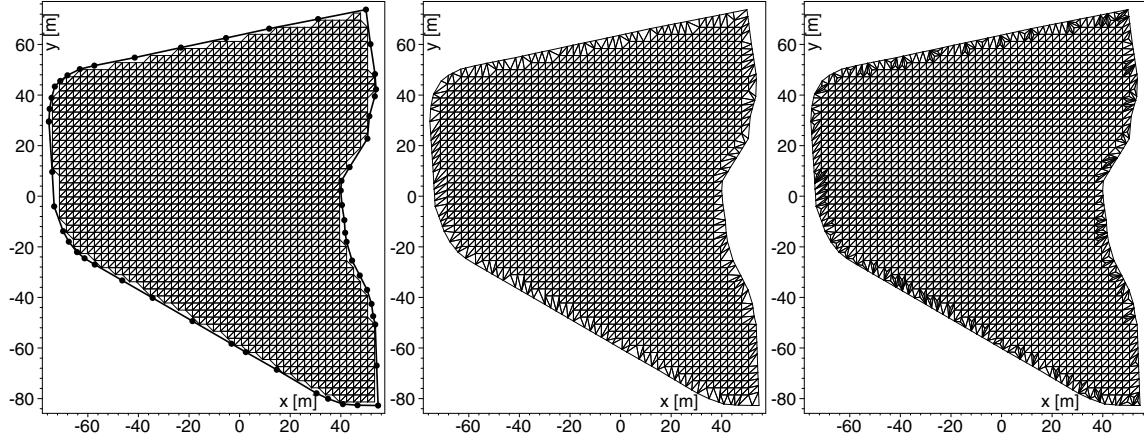


Figure 3: Triangulation

which defines the subsoil shape, was found using selected points from the slope's perimeter and reference points. There are a total of 38 points, which are shown in Figure 4. Six reference points are marked with a square and 32 points from the perimeter of the slope are marked with a cross. A thick black line indicates the intersection of the slope surface with the ground surface.

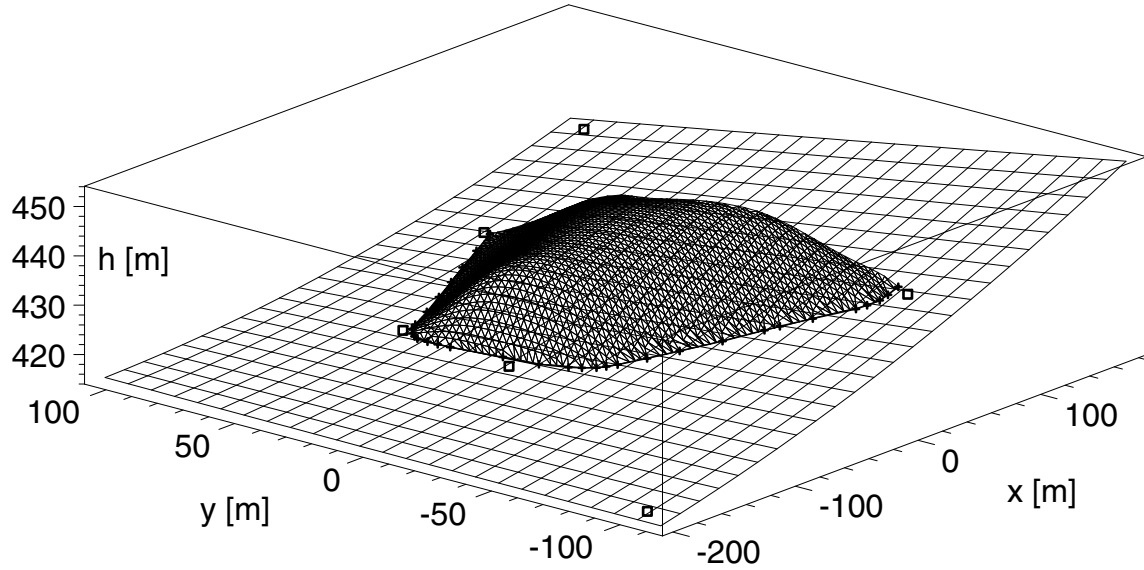


Figure 4: Subsoil and slope

The h function, see (4) interleaves the entered points with excellent accuracy. Its coefficient of determination is $R^2 = 0.9991$ and the p value calculated by the ANOVA method is even $p = 1 - 10^{-8}$.

3. Results

3.1. Displacement visualization

In the first step, the displacement vectors are plotted for the entire monitoring time, see Figure 5. These vectors are plotted with a thick black arrow and are compared to vectors corresponding to the slope gradient, which are plotted in dark gray, and with vectors corresponding to the subsoil slope, which are plotted in light gray. Identical color shades are also used to represent the hill and subsoil contours, which increase the clarity of Figure 5. Black squares indicate the starting positions of the moving points. A thick black line highlights the perimeter of the hill.

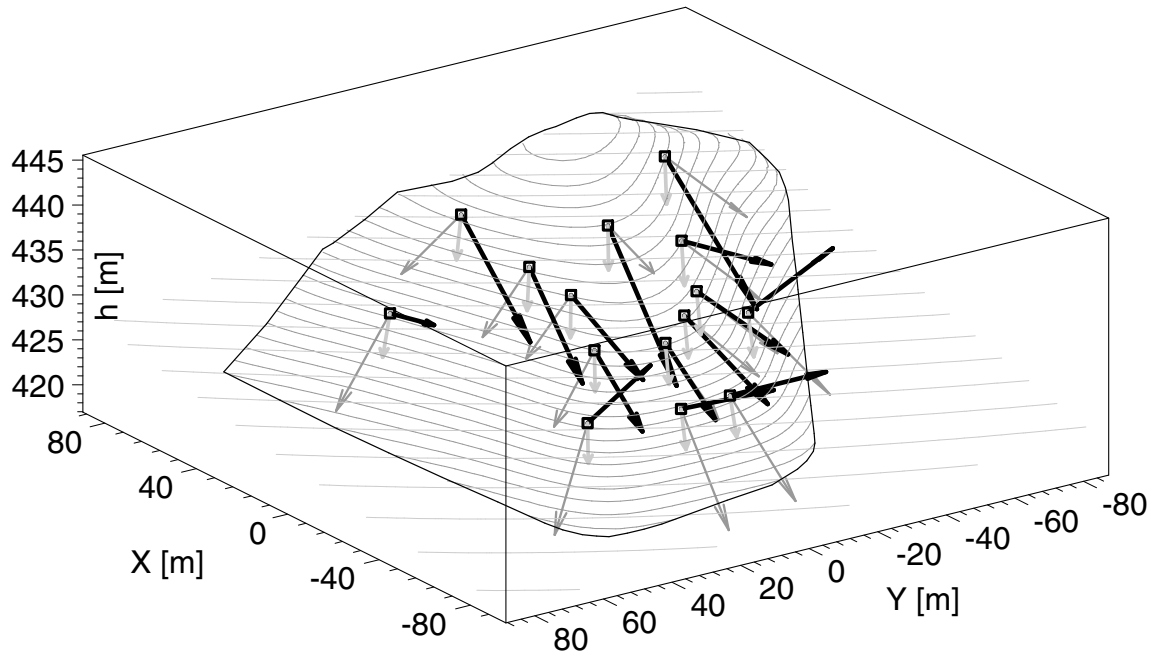


Figure 5: Displacement vectors – black, slope gradient – dark gray and subsoil gradient – light gray.

It can be seen from Figure 5 that the displacement vectors do not correlate with the slope gradient vectors. The correlation of the direction of displacement and gradient of the slope in the xy plane is 0.21 - the hill does not collapse. The correlation of the direction of displacement and incline of the subsoil in the xy plane is 0.25 - the hill does not move. Therefore, movements in the vertical direction and the xy plane will be examined separately.

3.2. Vertical displacement

First, the dependencies of the vertical displacement on the relative height of the slope of the subsoil are plotted for individual years, see Figure 6.

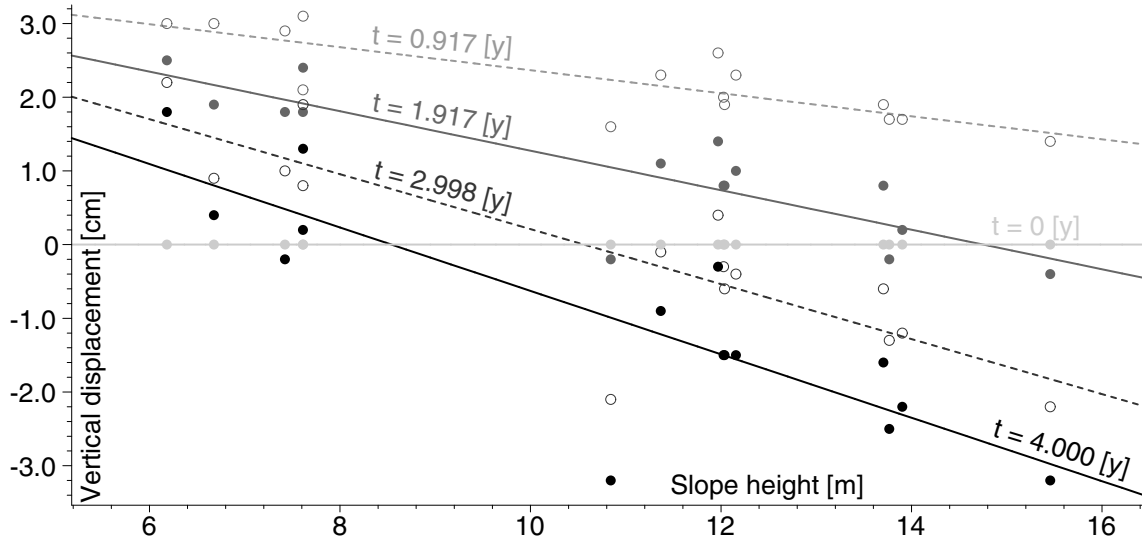


Figure 6: Dependences of vertical displacement on relative slope height h

It is very clear from this figure that for each year, it is possible to intersect the vertical displacement by a linear regression function of the relative slope height h . The coefficients of regression functions for individual years can be found by the method of least squares. The resulting regression functions, including the individual reliability coefficients and p values calculated by the method of analysis of variance, are given in Table 1.

time [year]	$\Delta h(h, t)$ [m]	R^2	p - value
0	0	1.0	1.0
0.91721	$3.92779 - 0.15618 h$	0.68234	$1 - 1 \cdot 10^{-10}$
1.91655	$3.95526 - 0.26810 h$	0.74713	$1 - 3 \cdot 10^{-10}$
2.99803	$3.93985 - 0.37299 h$	0.71784	$1 - 5 \cdot 10^{-10}$
4.000117	$3.67578 - 0.43037 h$	0.72088	$1 - 1 \cdot 10^{-10}$

Table 1: Vertical displacement depending on relative height and time.

It is clear from Figure 6 and Table 1 that a regression function $\Delta h(h, t)$ can interpolate the vertical displacement. This function should be zero for $t = 0$, $\Delta h(h, 0) = 0$ or for $h = 0$, $\Delta h(0, t) = 0$. A simple function that meets these requirements is:

$$\Delta h(h, t) = 0.54559 t h - 0.12271 h t^2 - 0.03369 t h^2 + 0.00656 t^2 h^2. \quad (5)$$

Its coefficients were calculated from the measured values by the method of least squares. For the calculated vertical displacement, the coefficient of determination is $R^2 = 0.72898$, and the value of p calculated by the ANOVA method is, $p = 0.59345$,

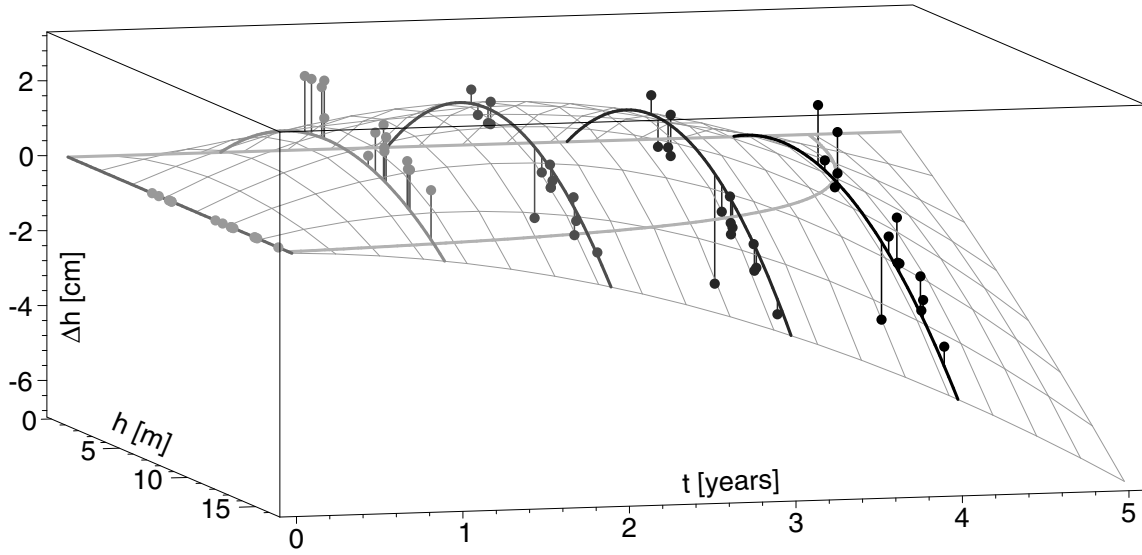


Figure 7: Dependence of vertical displacement on relative slope height h and time t

which are outstanding values. Figure 7 is a spatial representation of the function $\Delta h(h, t)$, (5), including measured values and error bars.

3.3. Horizontal displacement

For the sake of brevity and clarity, we will carry out a study of the overall horizontal shift for the entire period under review, i.e., for approximately five years. We will first draw the total displacement vectors and the slope and subsoil slope vectors, see Figure 8. Black circles indicate the initial positions of the moving points. Strong white arrows indicate the displacement vectors, dark gray arrows draw the slope gradient vectors, and the light gray arrows show the subsoil slopes. It is clear from Figure 8 that the displacement vectors do not correspond to the slope and subsoil gradients.

Therefore, we will try to find the vector field's regression function that will correspond to the vectors of the resulting displacement. Suppose that a vector field can be described by a function:

$$VF(x, y) = \left[\sum_{i=0}^3 \sum_{j=0}^{3-i} Ax_{i,j} x^i y^j, \sum_{i=0}^3 \sum_{j=0}^{3-i} By_{i,j} x^i y^j \right], \quad (6)$$

where the coefficients $Ax_{i,j}$ and $By_{i,j}$ are calculated using the least squares method. The displacement vectors of the individual moving points are stored in the Maple variable `rp`. The procedure for this calculation in the Maple environment is:

```
> rp2d:=map(u->map(v->v[1..2],u),rpa): vf:=op(expand((x+y+1)**3)): nf:=nops(vf);
> vf:=unapply(sum(op('i',vf)*a['i'],'i'=1..nf),x,y): Var:=[seq(a[i],i=1..nf)]:
> COL:=unapply(map(u->select(has,vf(x,y),u)/u,Var),x,y):
```

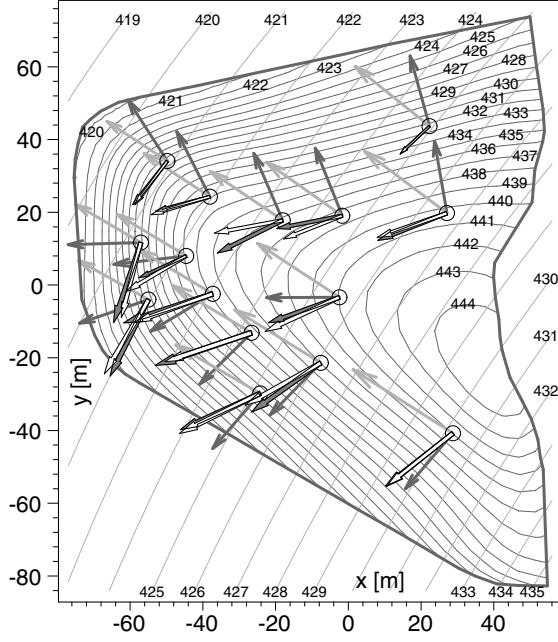


Figure 8: Measured and computed displacement

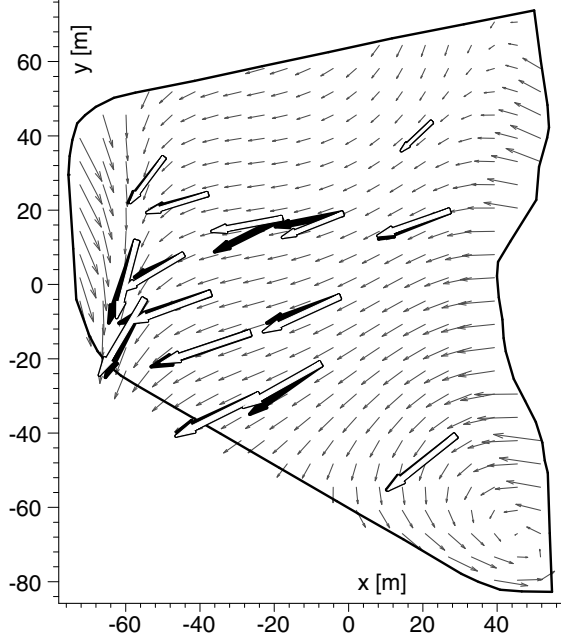


Figure 9: Measured and computed displacement and vector field

```
> M:=Matrix(map(u->COL(u[1][ ]),rp2d)):
> Bx:=Vector(map(u->u[2][1],rp2d)): By:=Vector(map(u->u[2][2],rp2d)):
> Ax:=LeastSquares(M,Bx); Ay:=LeastSquares(M,By):
> FX:=subs(seq(a[i]=Ax[i],i=1..nf),vf(x,y)):
> FY:=subs(seq(a[i]=Ay[i],i=1..nf),vf(x,y)):
> VF:=unapply([FX,FY],x,y);
```

$$VF := (x, y) \mapsto [-18.985 - 1.0051 \cdot 10^{-5} y^3 - 1.8326 \cdot 10^{-4} x^3 + 0.08193 y + 0.1250 x \\ + 3.7991 \cdot 10^{-3} y^2 - 5.0513 \cdot 10^{-3} x^2 - 1.4572 \cdot 10^{-4} x y \\ + 4.7957 \cdot 10^{-5} x y^2 + 3.2184 \cdot 10^{-5} x^2 y, \\ - 9.2791 - 2.70688 \cdot 10^{-5} y^3 + 1.7425 \cdot 10^{-4} x^3 + 0.1674 y - 0.1932 x \\ - 1.1561 \cdot 10^{-3} y^2 + 2.588 \cdot 10^{-3} x^2 - 2.6894 \cdot 10^{-4} x y \\ + 6.1792 \cdot 10^{-6} x y^2 - 8.0956 \cdot 10^{-6} x^2 y] \quad (7)$$

The calculated displacement vectors for the individual moving points are shown in Figures 8 and 9 by strong white arrows. In Figure 9, the vector field corresponding to the equation (7) is indicated by small arrows.

If the shape of the vector field function is known, it is possible to calculate this field's flow lines by numerical integration. These lines correspond to the direction of movement of the slope surface. The flow lines corresponding to the function (7) are shown in Figure 10. The vortex is visible at the coordinates [46.4, -69.1] in the lower right corner of this image. Since the slope surface cannot move in this way, it is appropriate to remove this vortex. Since there is no moving point in this vortex's vicinity, let us try to assume that such a moving point would be located right in the center of the vortex.

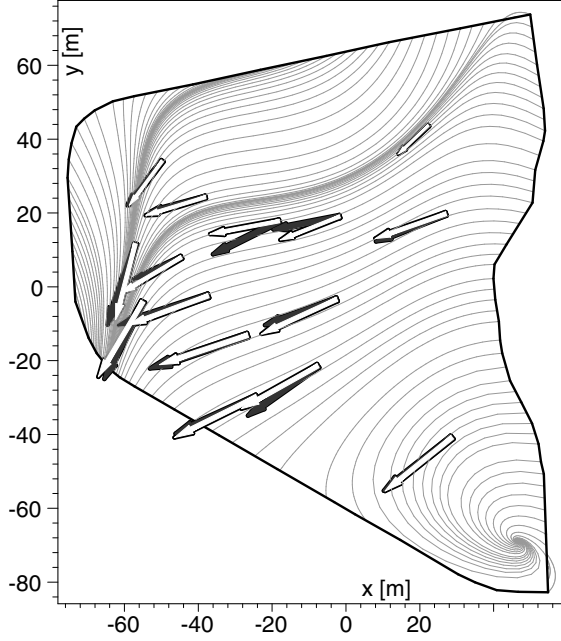


Figure 10: Flow lines of the original vector field

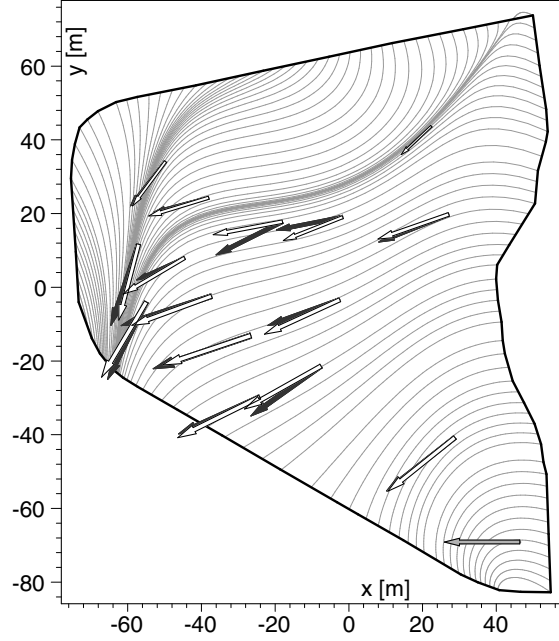


Figure 11: Flow lines of the amended vector field

Furthermore, it can be assumed that the vector of the total displacement could have a direction perpendicular to the nearest part of the slope circumference. We place a vector with the average size of the vectors of all moving points in the center of the vortex and orient it in the negative direction of the x -axis. So we add the vector $[-20.5, 0]$ to the variable `rp` and repeat the whole previous calculation. The flow lines of the complemented vector field are shown in Figure 11. A thick gray arrow indicates the new vector. As can be seen, the vortex has been removed.

It remains to be seen how much the new vector's addition altered the quality of the regression. This can be done by calculating the coefficient of determination and the p-value calculated by the ANOVA method. We perform calculations for absolute values and displacement vector arguments for the original and modified vector fields. The results are shown in Table 2.

	Original vector field		Amended vector field	
	R^2	p - value	R^2	p - value
Abs. value	0.710	0.984	0.700	0.991
Argument	0.990	0.960	0.960	0.954

Table 2: Regression quality for original and amended vector fields.

It is clear from Figure 11 that the flow lines are approximately perpendicular to the slope contour's right side. Therefore, in Figure 12, all lines forming the right side of the slope outline are drawn, and the light gray arrows indicate the perpendicular direction to the individual lines. Dark gray and medium gray arrows indicate the original and amended vector field's vectors going through to the separate line segments center points.

Figure 13 also supports the finding that both vector fields are mostly perpendicular to the contour's right edge, displaying the box graphs of the arguments of the directional vectors. The light gray corresponds to the normal vectors. The light gray corresponds to the original vector field, and the supplemented vector field is in dark gray.

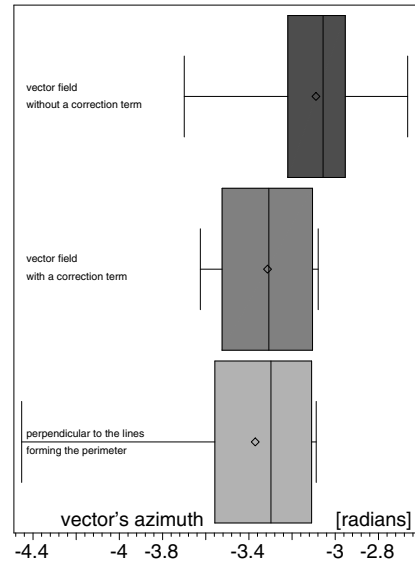
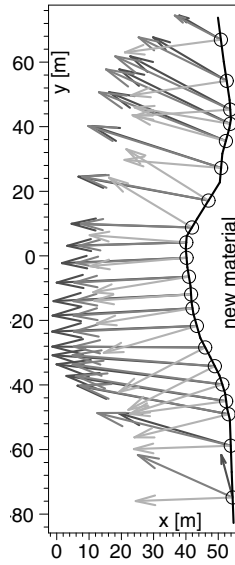


Figure 12: Vector fields and directional vectors of the active edge

Figure 13: Directions of vector fields and active edge normals

4. Conclusion

4.1. Surface movement in the vertical direction

The following facts follow from equation (5):

1. Positive vertical displacements in the entire slope area will cease after 4.45 years.
2. If the material layer is higher than 16.20 m, no positive vertical displacements will occur because its own weight compresses the slope material.
3. The maximum vertical displacement in the positive direction of 2.20 cm occurs after 2.00 years in a layer of material 7.30 meters thick.

4.2. Surface movement in the horizontal direction

From the properties of the vector field described by the equation (7) and the Figures 8–13 it can be deduced:

1. The slope as a whole does not slide on the subsoil.
2. Slope material does not slide.
3. The slope material is moved in the direction of the forces that arise when depositing a new material on the active edge of the slope. These forces are caused by the new material and the weight of moving vehicles.

Acknowledgement

The author would like to thank doc. Mgr. Ing. Magdalena Daria Vaverkova, Ph.D. and doc. Bc. Ing. Dana Adamcova, Ph.D. from Mendel University in Brno, who provided the information for processing as well as the suggestion that this might make an interesting topic.

References

- [1] *Parametry zemli 1990 (PZ-90.11) Reference document*. Military topographic department of the general staff of armed forces of the Russian federation, Moscow, 2014, available at: https://eng.mil.ru/files/PZ-90.11_final-v8.pdf, downloaded August 20, 2020
- [2] Gander, W., Gander, M. J. and Kwok, F.: *Scientific Computing - An Introduction using Maple and MATLAB*. Springer International Publishing, 2014, ISBN: 978-3-319-04324-1
- [3] Kettner, L., Kurt, M., Sylvain, P., Stefan, S. and Chee, Y.: Classroom examples of robustness problems in geometric computations. *Comput. Geom.* **40** (2008), 61–78